Journal of Building Engineering 15 (2018) 203–217

Contents lists available at ScienceDirect

Journal of Building Engineering

journal homepage: www.elsevier.com/locate/jobe

Plane and vaulted masonry elements strengthened by different techniques – Testing, numerical modeling and nonlinear analysis

Gehan Hamdy*, Osama Kamal, Osama Al-Hariri, Tarik El-Salakawy

Civil Engineering Department, Faculty of Engineering at Shoubra, Benha University, 108 Shoubra Street, Shoubra 11241, Cairo, Egypt

ARTICLE INFO

Keywords:
Masonry
Strengthening
Numerical modeling
Nonlinear analysis
Vault

ABSTRACT

This paper presents numerical modeling and nonlinear analysis of unreinforced masonry walls and vaults externally strengthened by different techniques. The aim of the research is to provide a simple and reliable calculation method to enable the design and structural evaluation of strengthening measures for masonry plane and arched structures. Numerical modeling by finite elements and nonlinear analysis are carried out using commercial software ANSYS12.0. In order to validate the adopted approach, an experimental program was conducted where unreinforced brick masonry walls and vaults were strengthened by several techniques and loaded until failure. Comparison of experimental and numerical results showed acceptable agreement. Furthermore, a parametric study is conducted to investigate and compare several strengthening configurations for unreinforced masonry vault in order to select the optimum solution. The numerical results are discussed and the deduced conclusions illustrate the applicability of the proposed approach as a practical and valid tool for design of strengthening interventions for contemporary or historic masonry elements and assemblages.

1. Introduction

Unreinforced masonry walls, arches and vaults constitute the load-bearing elements of many contemporary and historic structures worldwide. These structures are often subjected to deterioration and damage and may require strengthening. Any intervention strategy should be based on understanding of the behavior of the existing structure as well as its behavior after the proposed retrofit measures are made [1]. Linear analysis usually performed to simplify the analysis and design of masonry structures might underestimate the structural capacity of such constructions and hence the inelastic structural response is more adequate for representation of the structural behavior [2]. Nonlinear analysis is required for vulnerability assessment and proposing seismic retrofit schemes for traditional and heritage masonry structures [3,4]. The availability of an effective nonlinear tool for the seismic assessment of masonry structural elements is thus a crucial requirement.

This paper presents numerical analyses of non-strengthened and strengthened semicircular masonry arches, in order to evaluate the effectiveness of different carbon FRP (CFRP) strengthening proposals.

The main objective of the research is to investigate numerically the behavior of unreinforced masonry walls and vaults strengthened by different schemes in order to evaluate the effectiveness of the strengthening method and to enable proper design of such interventions. Finite element modeling and nonlinear analysis are conducted using commercially available computer software ANSYS v.12 [5]. The adopted modeling parameters, material characterization and nonlinear solution parameters are presented.

In order to validate the adopted numerical representation, an experimental program was conducted where unreinforced masonry walls and vaults were strengthened using several techniques. The studied techniques represent externally applied retrofitting methods for upgrading masonry vaults of moderate cost; namely steel reinforcement bars, ferro-cement layers and polymer mortar layers in addition to glass fiber reinforced polymer (GFRP) sheets [6]. The experimental and numerical results are presented and compared.

To demonstrate the useful application of the proposed numerical approach, a numerical study was conducted where several strengthening configurations for an unreinforced masonry vault were modeled. The numerical results are discussed to select the most efficient strengthening scheme.

* Corresponding author.
E-mail addresses: gehan.hamdy@feng.bu.edu.eg (G. Hamdy), osama.kamal@feng.bu.edu.eg (O. Kamal), osama.elhariri@feng.bu.edu.eg (O. Al-Hariri), tarek.abdelgalil@feng.bu.edu.eg (T. El-Salakawy).

https://doi.org/10.1016/j.jobe.2017.11.009
Received 18 October 2016; Received in revised form 16 November 2017; Accepted 17 November 2017
Available online 21 November 2017

2. Numerical modeling and nonlinear analysis of masonry elements

2.1. Approaches for modeling and nonlinear analysis of masonry

Masonry is a heterogeneous material with a complex, non-linear, anisotropic behavior due to the different material components and presence of mortar joints. The complex irregular nature of masonry construction makes accurate structural analysis a challenge. Linear elastic analysis commonly used in practice does not accurately estimate the ultimate response of masonry and should not be used to conclude their strength and structural safety margin. Nonlinear analysis is considered to give better description for the behavior and capacity of masonry structures in many cases [1].

To represent the heterogeneous and anisotropic nature of masonry construction using finite elements, different modeling strategies may be followed that are reviewed by Roca et al. [2]. Discretization of the structure can be performed using the following three approaches: (i) detailed micro-modeling, where masonry units and mortar joints are distinctly modeled as materials with different geometry and mechanical properties whereas the unit-mortar interface is represented by discontinuous interface elements accounting for possible crack or slip planes [7]; (ii) simplified micro-modeling, bricks are modeled by continuum elements while mortar joints are lumped in discontinuous interface elements [8]; (iii) macro-modeling, masonry is modeled as an isotropic continuum material characterized by different nonlinear softening laws in tension and compression [9].

Comparison of the three main modeling strategies for masonry conclude that although detailed micro-models are capable of addressing some of the complexities, their application is primarily restricted to small-scale structures with regular geometric forms [1,2]. The macro modeling (smeared, continuum or homogenized) is more practice oriented due to the reduced time and memory requirements as well as a user-friendly mesh generation, and describes the structural behavior with acceptable accuracy [10]. The smeared crack scalar damage models commonly used for reinforced concrete structures were also adapted for masonry historic buildings, where the damage is defined in a given point by a scalar value which defines the level of material degradation, and the cracking is considered as distributed along the structure [11].

Nonlinear analysis was conducted to explore the seismic behavior and detect the vulnerability of several heritage masonry structures. Peña et al. [12] presented a simple strategy of analysis for the seismic assessment of the Qutb Minar in Delhi, India using three different models for nonlinear static and nonlinear dynamic analyses. A detailed study of the Church of St. Constantine and Helen, Piraeus, conducted by Spyrakos et al. [13] included determining mechanical properties, structure construction details and the current condition of the structure as well as its dynamic behavior through in-situ and laboratory testing as well as through finite element analysis. Seismic vulnerability of a basilica in Italy was investigated by using a finite element model where the masonry non-linearity was represented by proper constitutive assumptions [14]. Ceroni et al. [15] studied the seismic vulnerability of heritage masonry building in Italy through non-linear static analyses using finite element model and estimate of the q-factor. D'D'Ambrisi et al. [3] addressed dynamic characterization and evaluation of the seismic performances of the medieval tower of Soncino (Cremona, Italy). Three-dimensional finite element models of the tower were used in the nonlinear finite element program ANSYS to carry out nonlinear static and dynamic analyses. Analytical models of the tower were calibrated on the results of the performed dynamic identification with ambient vibration tests.

Kamal et al. [16] investigated numerically the nonlinear behavior of unreinforced masonry. An experimental study was conducted in order to validate the accuracy of the adopted modeling and solution procedure by comparison with experimental results. Additionally, calculated numerical results were compared to published experimental results. The proposed numerical modeling was concluded to be suitable to study and understand the structural behavior of existing heritage structures and interpret the cracks or any structural problem encountered in it.

Betti et al. [17] investigated numerically the seismic behavior of unreinforced masonry buildings with reference to a two-story prototype tested on a shaking table using two numerical modeling approaches. The first numerical model was built by using the finite element (FE) technique, while the second one was built by a simplified macro-element (ME) approach. The results highlighted that the FE model was capable of reproducing with good confidence the experimental damages, while the macro-element model, due to the intrinsic hypothesis of rigid floors, is capable of predicting the collapse load, but not providing a satisfactory reconstruction of the actual collapse mechanism. The ME model underestimated the shear forces compared to the FE model [17].

A historical church and monastery in Italy were studied by Clementi et al. [4] using solid finite elements and the nonlinear behavior of masonry was taken into account by proper constitutive assumptions.

Regarding the material properties and constitutive relations to be used in the finite element analysis, analytical relations were proposed for masonry strength and deformation based on regression analysis of experimental data [18,19].

The ultimate compressive strength of masonry can be estimated as a function of compressive strength of brick (fb) and mortar (fm) evaluated by tests [20]. A simple linear relationship between the masonry and brick strength was proposed by Bennett et al. [21] with the compressive strength of masonry estimated as 0.3 times the brick compressive strength. Further analytical models for the prediction of compressive strength and deformation characteristics of masonry have been proposed by previous researchers [22,23].

Several authors have investigated the stress–strain relationships developed on uniaxial compression of masonry prisms and brick. Equations were developed for the estimation of the elastic modulus and stress–strain curves were derived for fired-clay brick masonry bound with different mortars using regression analysis of experimental data [24]. McNary and Abrams [20] noted that the relation between stress and strain under compression becomes increasingly non-linear as mortar strength lowers. Eurocode 6 [25] acknowledges that the stress–strain relationship of masonry in compression is nonlinear. The code permits the stress–strain curve to be taken as linear (up to 0.33 f'm) or as a parabolic rising curve (up to a strain of 0.002) and as a horizontal plateau up to 0.0035 of strain. Other authors describe the parabolic rising portion as part of a 'modified' Kent-Park model [18,23,26] consisting of a parabolic rising curve, a linear falling branch and a horizontal plateau. Kaushik et al. [18] also considered the ascending part of the masonry stress–strain curve as a parabolic curve by fitting to experimental data.

Masonry stiffness varies considerably with its compressive strength as evidenced by a wide range of values in the literature. Kaushik et al. [18] studied the uniaxial monotonic compressive stress–strain behavior and estimated the modulus of elasticity of bricks, mortar and masonry as 300, 200, and 550 times their compressive strengths, respectively. Kaushik et al. [18] found by linear regression that the elastic modulus of masonry bound with mortars of variable strength reached values of 250–1100 times the compressive strength. Most authors propose values of 700–750 [26] and 1000 for k as given by Eurocode 6 [25]. Costigan et al. [24] generated models for lime-mortar masonry deformability based on regression analysis of the experimental stress–strain data, and compared them with published models. Experimental tests were conducted by Radovanovic et al. [27] to determine the mechanical properties of masonry such as compressive strength, elasticity modulus, shear modulus and tensile strength of the masonry walls. Values of characteristic compressive strength obtained analytically and based on equations given in current European and American regulations are

larger than those of the tested walls. Experimentally determined values for the modulus of elasticity of the tested walls were found to be higher than those provided in these regulations [27].

2.2. Nonlinear modeling of strengthened masonry elements

For modeling masonry structures reinforced with external strengthening systems, the model should take into account the masonry itself, the type of reinforcement and the interaction between the masonry and the reinforcement. Different numerical modeling approaches for strengthened masonry elements were studied by researchers. The use of a three-dimensional structural model of the cracked masonry dome of the historical church of St. Anna in Poland [28] allowed detailed determination of the internal force distribution and the adoption of an appropriate repair and strengthening regime for this load-bearing structure. The designed strengthening construction works were based on using carbon tape and spiral steel rods system [28]. A traditional means for strengthening existing masonry buildings is by steel available in a variety of forms such as bars, cold-formed members, thin-walled sections or welded elements. Structural upgrade of a public school building was designed and implemented, and proved suited to conservation and upgrade of the building [29]. Non-linear analysis of masonry shear walls strengthened with steel bars is attempted using a proposed macro-model. The model is based on the so-called disturbed state, with a modified hierarchical single yield surface plasticity model accounting for a distinct behavior in tension and compression [30].

External strengthening of masonry elements and structures using fiber reinforced polymers (FRP) has gained wide acceptance [31]. The use of fiber-reinforced polymer (FRP) strips has been shown to improve the load-carrying capacity and deformations of masonry members subjected to out-of-plane loading. Externally applied GFRP reinforcement on one story buildings was experimentally proven to be reliable for the most severe earthquake accelerations without visual damage [32]. Covering only 20% of the external wall surface provided an easily placed and cost effective solution [32]. Experimental tests were conducted by Willis et al. [33] on clay brick masonry wallettes retrofitted with horizontal near-surface mounted (NSM) carbon FRP strips and subjected to horizontal bending. Mathematical models were developed to predict the moment at cracking and moment capacity for the specimens and were validated against the experimental results. Externally bonded grids were used by Papanicolaou et al. [34] for increasing the load-carrying and deformation capacity of unreinforced masonry wallettes of perforated fired clay bricks and solid stone blocks subjected to cyclic loading. The tested grids were open mesh structures comprising carbon, glass or basalt fibers and polypropylene or polyester, and the bonding agents were mortars of different compositions and epoxy resin [34]. The use of externally bonded grids was recommended as a promising solution for the structural upgrade of existing masonry structures [35].

One of the common seismic strengthening techniques for load bearing masonry walls, referred to as reinforced plastering mortar solution, consists of the addition of outer leafs (preferably on both faces of existing walls) made of premixed structural mortar or sprayed concrete reinforced with strengthening meshes (steel or fibreglass). Confined masonry walls were retrofitted using low-cost ferrocement and GFRP systems and subjected to vertical load and lateral reversed in-plane cyclic loading by El-Diasity et al. [35]. The proposed upgrading techniques improved the lateral resistance of the confined walls by 25–32% with significant increase in the ductility and energy absorption of the panel ranging from 33% to 85%. Additionally, collapse was significantly delayed by maintaining the wall integrity under large lateral deformations. Additionally, non-linear finite elements analysis was carried out using the computer package ANSYS [5]. A macro modeling approach was adopted, where the three-dimensional element Solid65 was chosen to represent masonry. The proposed model showed good agreement with the results of the laboratory tests for crack patterns and failure mechanisms for all models [35].

An innovative technique that enables the connection of several masonry components is stitching masonry through continuous flexible elements. It also conforms to the principles that govern the intervention on heritage structures: minimal intervention, compatibility, reversibility, respect of authenticity, matter conservation, control of the visual impact and possibility of recognizing the intervention. In an experimental study by Monni et al. [36], basalt fibers ropes of nominal diameter 4 mm were used as continuous flexible elements. The technique proved through the tests to be effective in improving the behavior against in-plane and out-of-plane loads.

Detailed micromechanical modeling was implemented for analysis of strengthened masonry elements, where masonry units, strengthening layer, mortar joints and interface planes are modeled with exact geometry and mechanical properties that are defined through laboratory tests [37]. Macro-modeling approaches were also applied for masonry panels reinforced with FRP strips which were modeled with elements having membrane stiffness and tension-only behavior and assumed perfectly bonded to the masonry [38], or using special constitutive material models for the masonry-FRP interaction [39]. Masonry panels externally strengthened with textile reinforced mortar were modeled by Basili et al. as an isotropic continuum material characterized by different nonlinear softening laws in tension and compression derived from experimental tests [40]. The mortar layer and embedded reinforcement were modeled as an equivalent linear elastic grid by plane elements considered perfectly bonded to the panel by Ceroni et al. [41].

Homogenized anisotropic material and smeared crack model were used for masonry vaults strengthened with FRP strips at the extrados. The FRP strips assumed fully bonded to the masonry were modeled as solid elements with anisotropic material properties [42], or as linear elastic and orthotropic until fiber tensile strength is reached and rupture of fibers occurred [43]. Numerical approaches to model the masonry-FRP interface behavior have been also proposed [44].

2.3. Adopted nonlinear material behavior and solution procedure

Within this research work, a macro-modeling approach is adopted, in which the masonry units and mortar joints are considered as homogenous continuum. The commercial computer software ANSYS V.12 is used for finite element discretization and for nonlinear analysis [5]. The eight-node solid isotropic element SOLID65 is used to model the nonlinearity of brittle materials. The nonlinear behavior of SOLID65 element is based upon the Willam–Warnke yield criterion [45], a constitutive model for the failure and tri-axial behavior of concrete materials that has been demonstrated to be suitable for masonry [46]. The element accounts for cracking in tension with a smeared crack analogy and crushing in compression with a plasticity algorithm. The stress–strain relationship has two phases: linear elastic behavior and nonlinear behavior after either of the specified tensile or compressive strengths is exceeded. Cracking or crushing occurs when any of the three principal stresses exceed the specified tensile or compressive strength at any of the eight integration points. Then, a plane of weakness is introduced in the principle stress direction, thus decreasing the global stiffness and simulating the formation of a crack [5].

3. Experimental program

In order to verify the numerical modeling approach, an experimental program was conducted within the research to compare the experimental results with those obtained numerically. The experimental program was performed at the Concrete and Composite Structures Laboratory of the Faculty of Engineering at Shoubra, Cairo, Egypt. It included testing of masonry wallets and vaults constructed using local clay bricks and strengthened by different techniques. Laboratory tests were also carried out to determine the mechanical properties for masonry units, mortar, masonry prisms and

strengthening materials [6].

3.1. Materials

3.1.1. Masonry units

The masonry units used were local commercial clay bricks (Misr Brick) with dimensions 250 × 120 × 60 mm. Three brick units were tested in compression until failure; and the obtained average compressive strength was 12.5 MPa.

3.1.2. Mortar

The mortar used for all experimental work was mortar type 1 in accordance with the Egyptian code for masonry structures (ECP 204-2005) [47]. The mix proportions for mortar were 1:3 cement: sand by volume, and w/c ratio of 0.5. Three mortar cubes of dimensions 100 × 100 × 100 mm were tested after 28 days in compression until failure. The average for compressive strength was 17.1 MPa.

3.1.3. Steel reinforcement

The used steel reinforcement was mild steel smooth bars (Grade 240/350) with diameter 6 mm and having yield stress (*fy*) of 240 MPa, ultimate tensile strength (*fu*) of 350 MPa and modulus of elasticity (*Es*) of 200 GPa.

3.1.4. FRP sheets

The used FRP sheets were E-glass fiber woven roving EWR600, having fiber diameter 17 μm, density 600 g/m^2, breaking strength 3800 MPa and modulus of elasticity 75 GPa. The FRP sheets were adhered with polyester resin; the resin was mixed with hardener to accelerate the setting time with volume ratio 2 cm^3 for each litre of polymer material.

3.1.5. Ferro-cement wire mesh

For ferrocement layers used for strengthening, expanded galvanized wire mesh was used with wire diameter 1.5 mm, grid size 25 mm, weight 630 kg/m^3 (0.945 kg per square meter). The wire mesh is made of mild steel (Grade 240/ 350) having yield stress *fy* 240 MPa, ultimate tensile strength *fu* 350 MPa and modulus of elasticity *Es* 200 GPa.

3.1.6. Polyester mortar

The mortar used for repair consisted of sand and polyester polymer in the ratio 3:1 by volume; hardener is added to accelerate the setting time with ratio 2 cm^3 for each liter of polymer material. Cubes with dimensions 70 × 70 × 70 mm and 70 mm- diameter cylinders with height 150 mm were prepared and tested to determine the compressive and splitting tensile strength. The average compressive and tensile strength for polyester mortar was 71.1 MPa and 4.3 MPa, respectively.

Five standard masonry prisms were prepared as specified by Egyptian code [47], and tested in compression to evaluate the masonry prism compressive strength. The average compressive strength of the masonry prisms ($f'm$) was 4.4 MPa. This experimentally determined value is close to the value of 0.3 brick strength as suggested by Bennett et al. [21].

3.2. Construction of the tested walls and vaults and strengthening schemes

Six masonry panels were built using the local clay bricks laid in ten courses in running bond with mortar joints 10 mm thick. The dimensions of each wallet were 700 × 700 × 120 mm. Two wallets were not strengthened and four wallets were strengthened by adhering 200 mm wide strips of GFRP on both sides using polyester resin, as shown in Fig. 1. The surfaces were treated with a primer coating to reduce porosity of the masonry before adhering the GFRP.The strengthening scheme and performed testing procedure were similar to those reported in the literature [39].

Twelve unreinforced masonry vaults were constructed having half brick ring thickness (120 mm) and the dimensions shown in Fig. 2. Three vaults were not strengthened to serve as control samples, while nine were strengthened on the extrados at locations chosen near the hinges expected to occur using four different techniques, as illustrated in Fig. 3. For three vaults, steel bars of length 50 cm and diameter 6 mm were inserted as near surface reinforcement, as shown in Fig. 3(a). Two vaults were strengthened using externally adhered GFRP Roving 600; two vaults were covered with sand polyester mortar in order to provide tensile strength to the external face of the vault. The last two vaults were strengthened by ferro-cement layer composed of a mesh of galvanized steel wire having thickness of 1.5 mm, which is fixed to the masonry vault after spatter dashing it by nails every 100 mm in both directions, then the mesh is covered with cement mortar layer to a total thickness of 20 mm. Strengthening of vaults by polyester mortar, GFRP and ferro-cement layers are illustrated in Fig. 3(b), (c) and (d), respectively. The walls and vaults were left to cure for 28 days before testing. The strengthened vaults are shown in Fig. 4.

3.3. Test setup and testing procedure

The masonry wallets were tested by diagonal compression test as per ASTM E519-02 [48]; the test setup is composed of two steel loading shoes fixed on two opposite corners on the wallet where the load was applied by a hydraulic jack on the top, as shown in Fig. 6(a). The tests were carried under displacement control in order to capture post-peak response of the specimens. Measurement of vertical deformation was by means of LVDTs attached to the centerline of one face of the wallet. For the masonry vaults, the vertical loading was made by means of a steel tank 1000 × 1000 × 1000 mm, filled with calibrated and saturated sand, with maximum capacity of about 20 kN. The displacement is measured using a digital dial gage placed at the vault intrados middle point, as shown in Fig. 5(b).

3.4. Experimental results

For the masonry wallets and vaults loaded until failure, the failure loads are listed in Tables 1 and 2, respectively, and the load displacement curves are given in Figs. 6 and 7, respectively. The failure mode for the unstrengthened wallets W1 and W2 showed a typical diagonal tension crack, extending from the upper tip to the lower tip of the wall, as shown in Fig. 8(a), and the average failure load was 81.3 kN. For the FRP-strengthened wallets, failure of wallets W3, W4, W5 was by crushing of the top part, Fig. 8(b), and for wallet W6 debonding and splitting of the FRP sheet and a vertical crack occurred, as shown in Fig. 8(c). The average failure load for FRP strengthened walls was 221 kN.

The experimentally determined failure loads for the tested vaults, given in Table 2, indicate that the control vaults had average failure load 8 kN, also the average failure loads were 15 kN, 12.63 kN, 12.56 kN and 9.55 kN for vaults strengthened by FRP, steel reinforcement, ferro-cement layer and polymer mortar layer, respectively. The load displacement curves for all vaults, given in Fig. 7, indicate that the strengthening increased the stiffness of the vaults, and caused the final displacements to be less than those of control vaults. Failure of the unstrengthened control vaults V1, V2 and V3 occurred when three hinges were formed, two at the extrados and one at the intrados, as shown in Fig. 9(a). The failure loads indicated that the strengthening using steel reinforcement, FRP and ferro-cement wire mesh increased the ultimate loads to 150%, 190% and 150%, respectively. The modes of failure for vaults strengthened with polyester mortar and by GFRP sheets are shown in Fig. 9(b) and (c), respectively. The loading on masonry vaults in existing buildings is usually uniform and symmetric, and typical position for cracks and hinges causing failure are expected. The two vaults strengthened with polyester mortar failed to transmit the crack outside the strengthened zone and slightly improved the failure load with 118%. The other strengthening schemes succeeded to

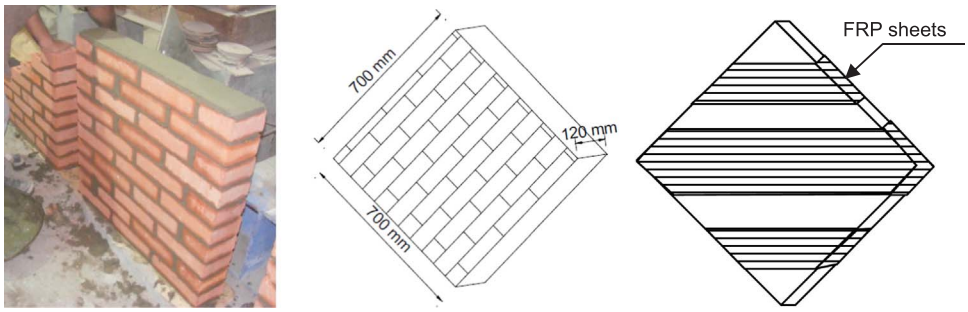

Fig. 1. Masonry wallets dimensions and strengthening scheme.

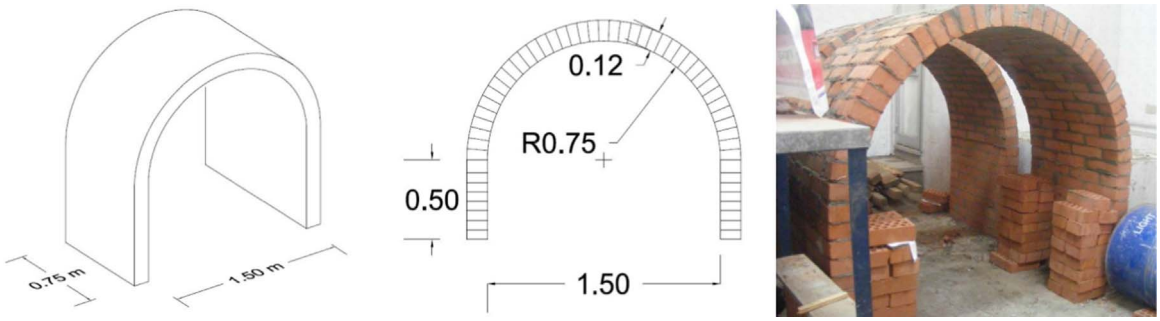

Fig. 2. Masonry vaults dimensions and construction.

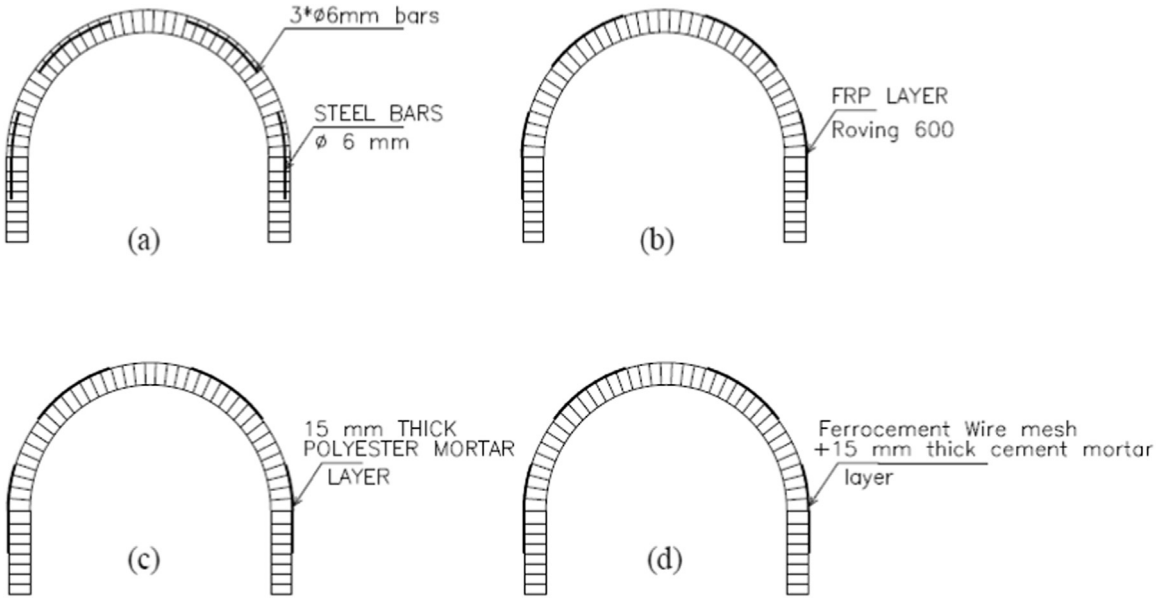

Fig. 3. Strengthening schemes for masonry vaults a) steel reinforcement, b) FRP sheets, c) polyester mortar layer, d) ferro-cement wire mesh.

transmit the crack formed on the control samples away from this position to the unstrengthened location.

3.4.1. Discussion of the experimental results

The experimental results demonstrated the efficiency of using externally bonded GFRP sheets for strengthening unreinforced masonry wallets and vaults. The obtained results show that the strengthening by using FRP delayed failure, nearly doubled the failure load and prevented the formation of diagonal cracks observed in the control samples. The final displacement shown in Fig. 6, increased from 5 mm for control samples to an average of 9 mm for strengthened wallets, indicating that the proposed strengthening increased the ductility of the tested samples.

The experimental results for vaults show variation between masonry vaults of the same strengthening type. Also, the load-displacement curves for vaults show drops and non-uniformity, probably due to the non-homogeneity of masonry in general and the rough loading process. Experimental results for vaults showed that using steel reinforcement and ferro-cement layers increased the ultimate load by an average of 60% and 56%, respectively. Using polymer mortar was the least effective technique, giving only 19% increase. The use of externally adhered FRP sheets gave nearly double the strengthening level and better failure mode, in addition to its excellent strength-to-weight ratio, easy installation and the relatively low cost for GFRP composites.

The obtained experimental results demonstrate also that the selected position of applied strengthening succeeded in closing the tension cracks at the location observed in the control vaults and moved the formed hinges causing the vault failure away from the location in the unstrengthened case. However, ductility was not improved since the strengthening was not provided to the whole vault but was only partial.

Fig. 4. Vaults after strengthening by a) ferro-cement wire mesh, b) GFRP sheets c) polyester mortar.

Thus, there were still brittle failure zones causing the observed brittle failure behavior.

The results are similar to those obtained by Oliveira et al. [49] who demonstrated that FRP sheets externally applied on the extrados of masonry vaults significantly increased the load-carrying capacity and modified the collapse mechanism. Mahini [42] demonstrated that application of FRP strips over the intrados and extrados of the cross vaults can prevent the cracks opening and the formation of hinges prior to collapse of the structure. Valluzzi et al. [50] concluded that proper location of carbon FRP strips used to strengthen brick masonry vaults can improve the vaults safety [50].

4. Numerical verification

For verification of the proposed modeling procedure, numerical modeling and nonlinear analysis were made for the experimentally tested brick wallets and vaults under the loading conditions of the experiments in order to demonstrate the capability of the approach in representing the structural response.

4.1. Numerical model

The experimentally tested walls and vaults were numerically modeled in a macro modeling strategy using the commercial software, ANSYS V.12 [5]. The modeling approach has been previous applied to unstrengthened masonry elements and managed to describe efficiently the behavior and explain the cracks observed in several historic masonry structures [16]. Masonry material (brick and mortar) is modeled using three-dimensional solid elements, SOLID 65, having eight nodes with three translational degrees of freedom at each node. The masonry is modeled as an isotropic material with homogenized properties characterized by different nonlinear softening laws in tension and compression. This type of material (MISO) uses the Von Mises yield

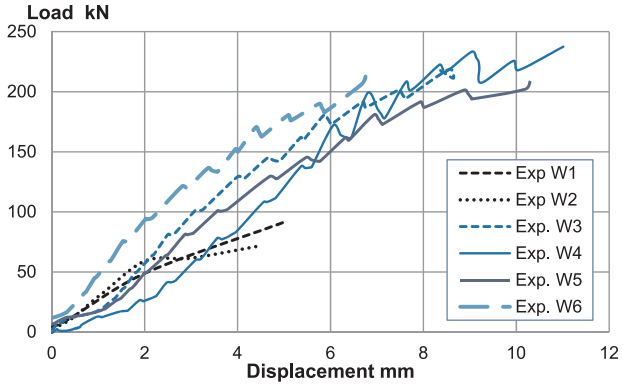

Fig. 6. Load-displacement curves for the tested masonry wallets.

Table 1
Failure loads of masonry wallets.

Wall ID	Failure load Pu (kN)	Increase of Pu than control %
W1	91.4	–
W2	71.2	–
W3	218.2	168%
W4	237.5	192%
W5	209.0	158%
W6	221.3	172%

Fig. 5. Test setup for a) wallets and b) vaults.

Table 2
Failure loads of masonry vaults.

Vault ID	Strengthening technique	Failure load Pu (kN)	Increase of Pu than control %
V1	Control	7.50	–
V2	Control	7.90	–
V3	Control	8.30	–
V4	Steel Reinforcement	13.50	168%
V5	Steel Reinforcement	12.11	151%
V6	Steel Reinforcement	12.29	153%
V7	GFRP	13.91	173%
V8	GFRP	16.04	200%
V9	Polymer mortar	10.10	126%
V10	Polymer mortar	9.00	112%
V11	Ferro-cement	13.00	162%
V12	Ferro-cement	12.00	150%

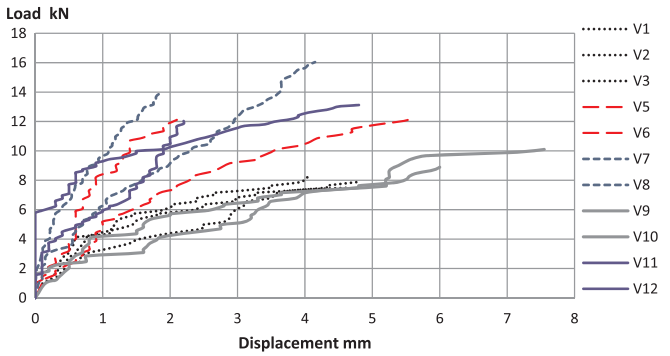

Fig. 7. Load-displacement curves for tested masonry vaults.

criteria coupled with an isotropic work hardening assumption. Multilinear isotropic hardening material is used to simulate the masonry and the strengthening mortar layers, describing the material behavior by a piece-wise linear total stress-total strain curve, starting at the origin, with initial slope corresponding to the elastic modulus of the material. The user defines the material tensile strength, compressive strength, and shear transfer coefficient which ranges from zero to 1.0. There are different suggestions for this coefficient in the literature, the suggest values for masonry by Sandeep et al. [51] were 0.3 and 0.6 for open and closed cracks respectively. When the solution converges to the cracked state, the modulus and consequently the stiffness normal to the crack face is set to zero. In the present study, the values assumed for the elastic modulus and the compressive strength of masonry were determined experimentally through uniaxial compression tests made on masonry prisms [6]. The stress strain curve was experimentally determined from the masonry prism tests. The value adopted here for modulus of elasticity for local masonry was experimentally determined to be about 150–200 times the prism strength of masonry. The masonry tensile strength is assumed 10% of the compressive strength according to Kaushik et al. [18] and ECP204- 2005 [47].

To simulate the steel reinforcement and ferro-cement wire mesh as well as the FRP layers, bilinear isotropic hardening material was used and option (BISO) uses the Von Mises yield criteria coupled with an isotropic work hardening assumption [5]. The material behavior is described by a bilinear stress-strain curve starting at the origin with positive stress and strain values and initial slope taken as the elastic modulus of the material. At the specified yield stress, the curve continues along a lower slope defined by the tangent modulus.

The meshes for unstrengthened and strengthened walls are shown in Figs. 10(a) and 11(a), respectively. Modeling for unstrengthened vaults and vaults strengthened by all techniques are shown in Fig. 12.

4.2. Material properties

The material properties of masonry and the strengthening materials are taken as follows [6].

a) Masonry: compressive strength $f'm$ = 4.47 MPa, modulus of elasticity Em = 625 MPa, weight density = 16 kN/m^3, Major Poisson's ratio = 0.15, tensile strength = 0.447 MPa
b) Steel reinforcement: yield stress = 240 MPa
c) FRP: ultimate tensile strength = 3800 MPa, modulus of elasticity = 75,000 MPa
d) Ferro-cement steel wire mesh: yield stress = 240 MPa

4.3. Nonlinear analysis parameters

The stress-strain relations for masonry and FRP were specified based on experimentally evaluated properties [6]. The loading of the model was similar to that conducted in the experimental program. An incremental load was applied over the vault crown at the midspan. The self-weight is also included in the analysis. For nonlinear analysis, iterative solution is adopted with load applied at increments. Nonlinear static analyses are performed and the Newton– Raphson iteration method is adopted by activating the energy norm criterion to check the convergence at each time step. The load is applied at increments; within each load step, the computer program may perform several substeps in which equilibrium iterations are made until convergence criteria are satisfied and a converged solution is reached.

The coefficients and parameters for nonlinear analysis are assigned the following values [6].

– Shear coefficient along opening cracks (ShrCf-pO) = 0.2
– Shear coefficient along closed cracks (ShCf-Cl) = 0.8

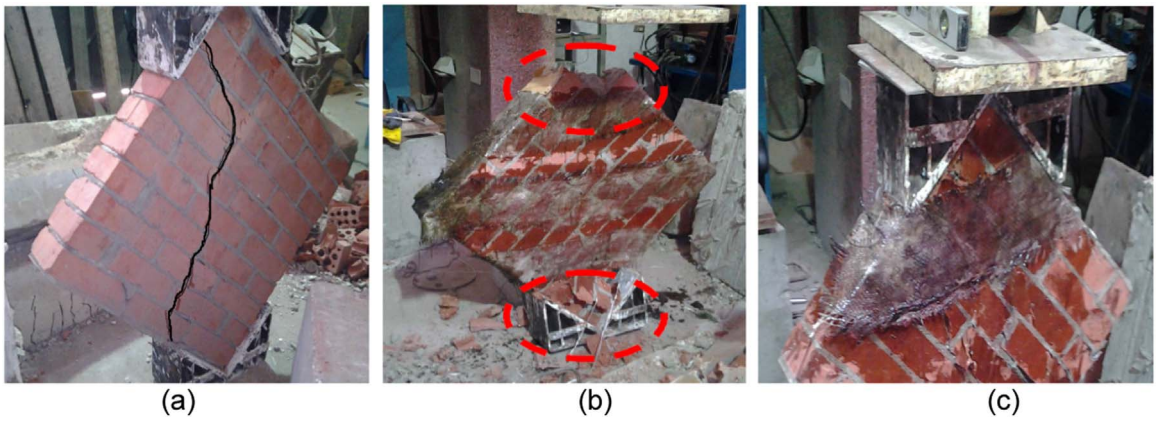

Fig. 8. Wallets failure mode a) unstrengthened, b) and c) wallets strengthened by GFRP.

Fig. 9. Failure of masonry vaults a) unstrengthened, b) vaults strengthened by polyester mortar and c) vaults strengthened by GFRP.

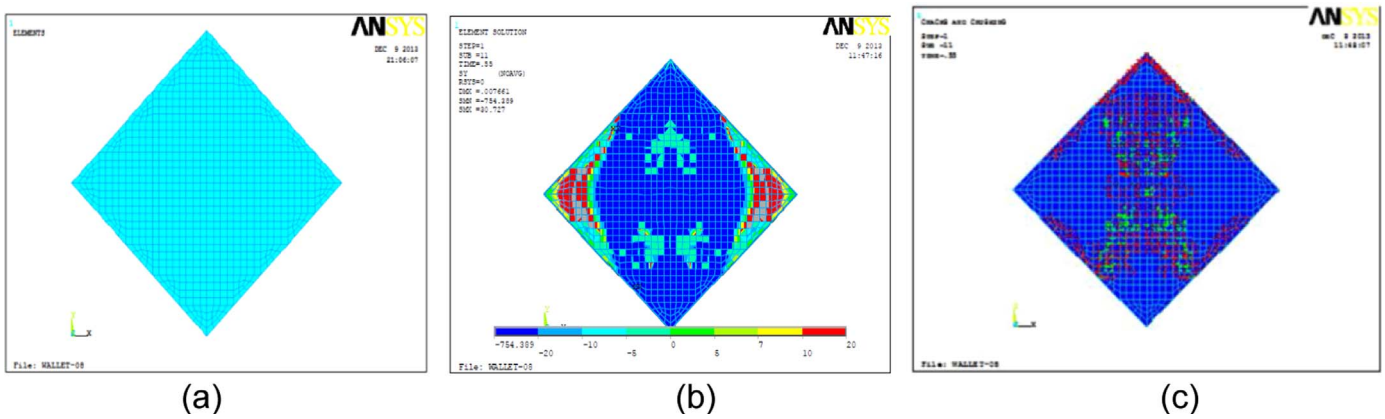

Fig. 10. Unstrengthened masonry wall: a) model, b) stresses (S_yx10^{-2} MPa) and c) cracks.

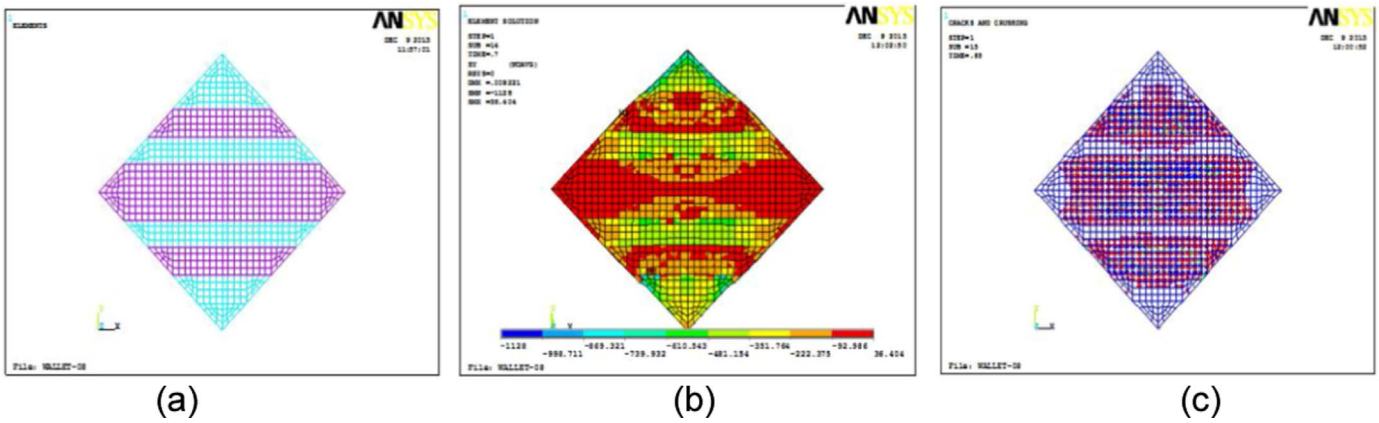

Fig. 11. FRP-strengthened masonry wall: a) model, b) stresses (S_yx10^{-2} MPa) and c) cracks.

- Tension limit, cracking limit (UnTensSt) = 0.425 MPa
- Compression limit, crushing limit (UnCompSt) = 4.25 MPa
- Number of load substeps solution = 10
- Number of equilibrium iterations = 25
- Convergence criteria: Newton-Raphson (displacement control)

5. Numerical results and comparison with experimental results

5.1. Failure loads and load-displacement relations for walls

The failure loads predicted numerically for the wallets are given in Table 3, compared to the average experimentally determined values. The load-displacement curves for the unstrengthened walls and for GFRP-strengthened walls are shown in Fig. 13. The numerically determined load displacement curves are observed to match with the experimental curves. The numerically predicted load displacement relation will also result maximum loads and displacements quite close to the experimental values.

5.2. Stresses and crack patterns for walls

The numerically evaluated stresses in unstrengthened and strengthened walls are shown in Figs. 10(b) and 11(b), respectively. The crack pattern at failure for the unstrengthened wall, presented in Fig. 10(c) shows longitudinal cracks from tip to tip. For the strengthened wall, cracks formed due to crushing at the top part of the wallet as shown in Fig. 11(c); also, cracks occurred between the brick elements and the FRP sheets, indicating that the stability of the wall was

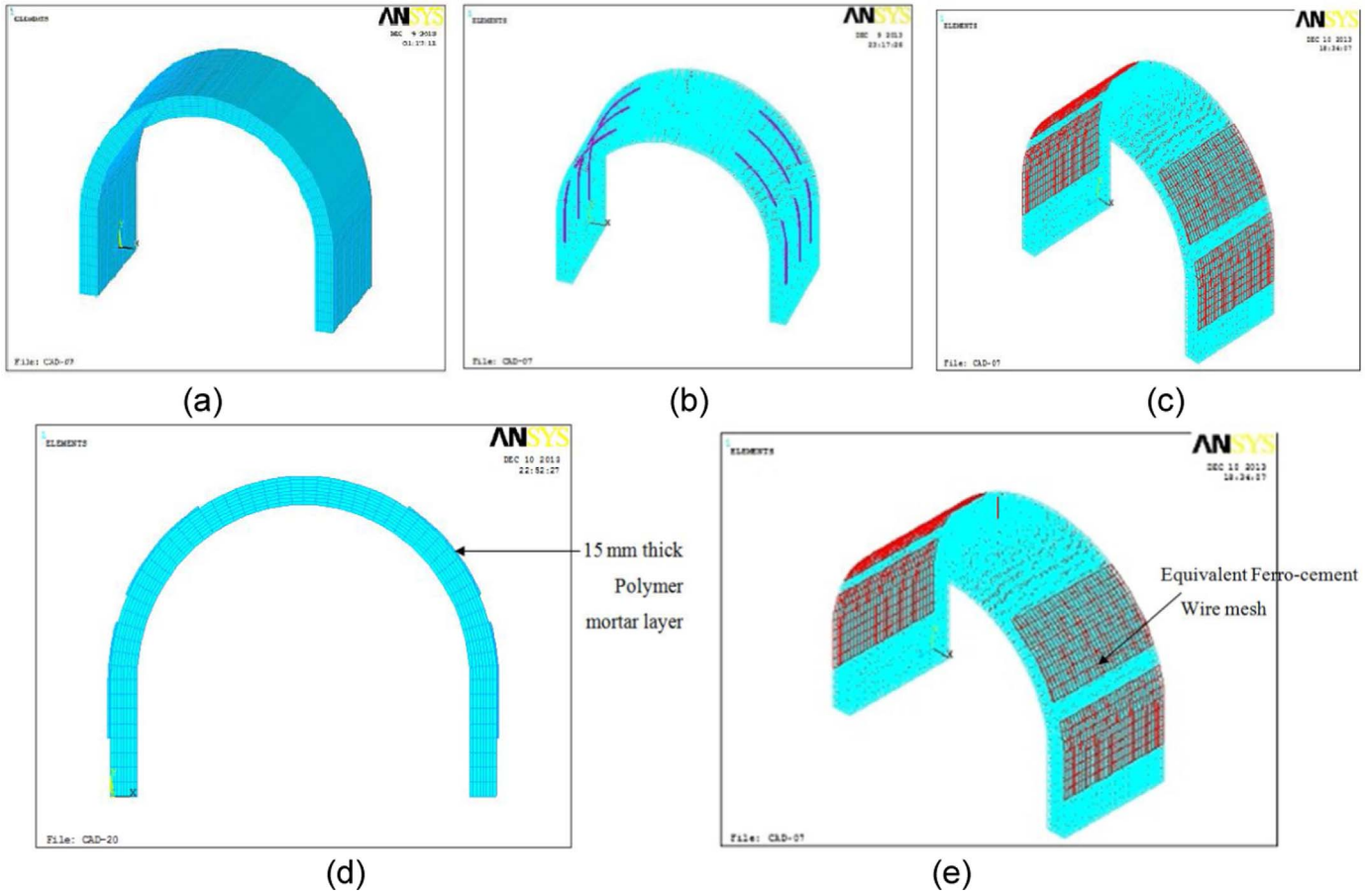

Fig. 12. Numerical model for a) control vault, b) vault strengthened by steel bars, c) vault strengthened by GFRP sheets, d) vault strengthened by polyester mortar layer and e) vaults strengthened by ferro-cement wire mesh.

Table 3
Numerical and experimental failure loads for walls and vaults.

Type	ID	Numerical failure load (kN)	Experimental failure load (avg.) (kN)
Unstrengthened wall	W1,W2	100	81.3
FRP-strengthened wall	W3,W4,W5,W6	225	221
Unstrengthened vault	V1,V2,V3	8.0	7.9
Vault strengthened by steel reinforcement	V4,V5,V6	13.5	12.65
Vault strengthened by GFRP sheets	V7,V8	14	15
Vault strengthened by polyester mortar	V9,V10	10	9.55
Vault strengthened by ferrocement layer	V11,V12	13	12.5

maintained through the confinement provided by FRP having development length. Failure modes predicted numerically agree with the experimental failure modes observed in Fig. 8(a) and (b).

5.3. Failure loads and load-displacement relations for vaults

Failure loads predicted numerically for all vaults are given in Table 3, compared to the experimentally determined values (average value), and show good agreement. Load-displacement curves for the strengthened vaults are shown in Fig. 14. Comparison with the experimentally determined curves reveals acceptable match for the first and last thirds of the curves but the middle third shows deviation from the experimental curves.

5.4. Stresses, crack patterns and failure modes for vaults

The crack pattern for the unstrengthened vault, shown in Fig. 15, indicate failure by formation of three hinges; the same as was observed experimentally. The numerical results for stresses and cracks in the vaults strengthened using reinforcement steel bars, FRP sheets and ferro-cement wire mesh are shown in Figs. 16 and 17. These vaults produced a mode of failure where the crack occurred between the two strengthened zones. For the vault strengthened with polymer mortar, the cracks occurred at the same locations as the control vault.

5.5. Comparison between numerical and experimental results

Numerically predicted ultimate failure loads and displacements at failure were very close to experimental results, which demonstrate the accuracy of the proposed numerical models. In most cases, the load-displacement curves show acceptable match for the first and last thirds of the curves but the middle third shows differences between numerical and experimental curves. This may be attributed to non-homogeneity of the experimental samples where defects or weak joints may cause stress concentrations. The numerically predicted cracking patterns and failure modes were quite identical to those observed experimentally.

6. Numerical study

6.1. Case studies description and modeling

A numerical study was inducted to demonstrate the significance of

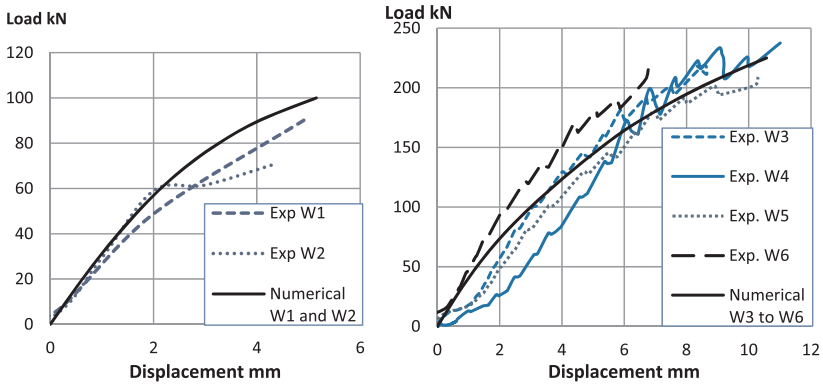

Fig. 13. Load-displacement curves for a) unstrengthened and b) FRP-strengthened walls.

the present work in facilitating design and optimisation of strengthening for unreinforced masonry vaults. Numerical modeling and nonlinear analysis was performed for a masonry vault having the same material and dimensions of the previous study, strengthened with externally applied steel bars, GFRP sheets and CFRP strips with various length, amount and location. Steel reinforcement was 6 mm diameter bars of mild steel (yield stress 240 MPa) or using 12 mm diameter bars of high strength steel (yield stress 360 MPa), the bars placed at spacing 250 mm or 125 mm. FRP strengthening was made using one or two layers of GFRP sheets having the previously stated properties. Also, CFRP strips were used of width 50 mm, thickness 1.2 mm, tensile modulus 165 GPa, ultimate tensile strength 2800 MPa and maximum strain 0.015.

Full length reinforcement was placed separately at the intrados or at the extrados. Then, symmetrical partial length reinforcement was placed at the extrados or at the intrados at specific locations based on the failure mode of the unreinforced vault, to cover 25%, 50% and 75% of the surface area as shown in Fig. 18. Additionally, full and partial strengthening was considered simultaneously at the intrados and extrados. The load was applied on the vault crown and increased until failure. The ultimate load of the vault and its failure mode and failure mode are determined for each case.

6.2. Numerical results and discussion

The numerically evaluated maximum vertical load carried by the vaults strengthened fully with the different materials are given in Table 4, the results for all vaults are summarized in Figs. 19–21 for the different strengthening schemes of steel bars, GFRP laminates and CFRP strips, respectively. The finite element model, stresses and cracking pattern of vaults with full steel and CFRP strengthening simultaneous at the extrados and intrados are shown in Figs. 22 and 23, respectively.

Numerical results show that all strengthening placed at the vaults intrados result in higher peak load values compared with the placement at the extrados for all the considered schemes. Similar observation was also made through numerical study by Basilio et al. [52] for CFRP strengthened masonry arches, where the same quantity of reinforcement, placed only at the external surface of the arch presents lower peak load when compared with the intrados reinforcement. Slightly higher load capacity is gained for simultaneous extrados and intrados strengthening for steel reinforcement and no gain for FRP strengthening.

Increasing the steel bars diameter has minor effect on increasing the vaults ultimate load, increase is only 5–7% although the area of steel is nearly tripled. However, using the bars of the same diameter bars at

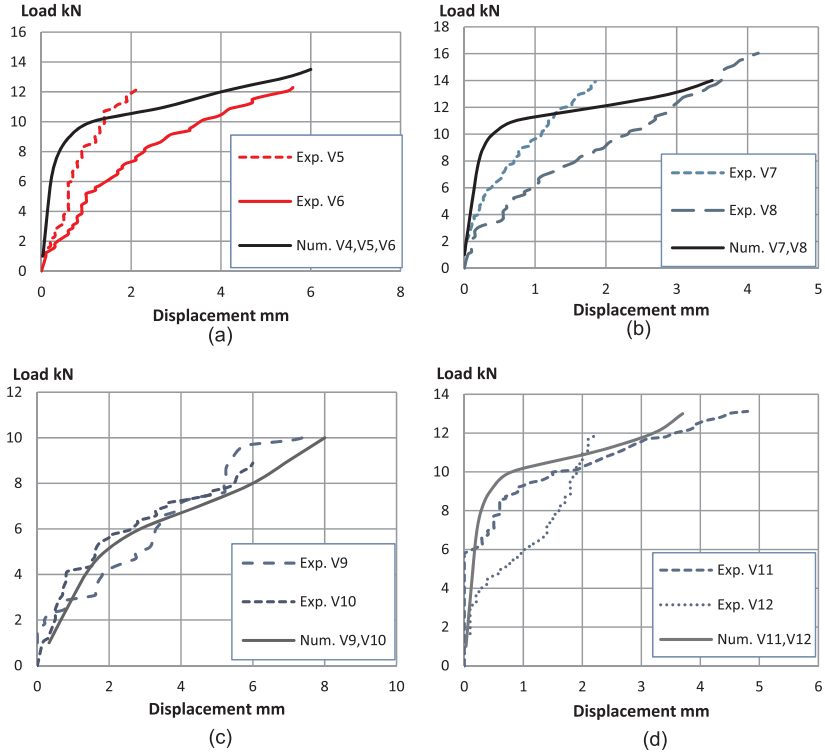

Fig. 14. Load-displacement curves for vaults strengthened by a) steel reinforcement bars, b) GFRP sheets, c) polyester mortar layer and d) ferro-cement wire mesh.

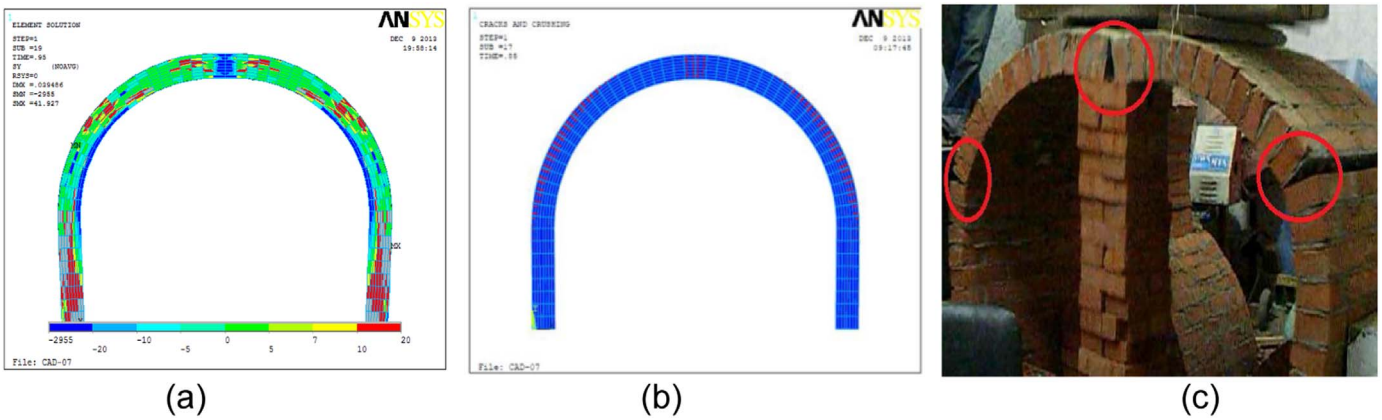

Fig. 15. Unstrengthened vault a) stresses Sy (x10^{-2} MPa), b) numerical crack pattern and c) experimental failure mode.

half spacing causes more evident increase in vault capacity of about 10–20%. Therefore, when designing strengthening elements it is better to intensify the distribution rather than increase the amount. Similarly, using two layers of GFRP sheets shows nearly no increase compared to one layer results, only 2–8% increase for full strengthening.

The location of strengthening has the most pronounced effect on increasing the ultimate load and improving the failure mode rather than amount of strengthening. Partial strengthening of 25%, chosen to be merely at the expected hinges, caused increase of the vaults ultimate load of 50–75% over the unstrengthened vault, which is a small increase compared to higher coverage for all schemes. Also the failure hinges were at the same locations as the unstrengthened vault and the cracks showed similar distribution. This may be explained by insufficient developed length which decreased the efficiency of the strengthening. Partial strengthening of 50% at the selected locations gave better results. Very high increase in the ultimate load was obtained for 75% coverage for intrados or simultaneous extrados and intrados steel bars to reach 3.25–5.25 times peak load of the unstrengthened vault and even higher peak loads for GFRP (4.6, 6.6 and 7.6 times for intrados, extrados and simultaneous, respectively).

Superior strengthening was attained by using GFRP on the vault intrados over steel reinforcement. Full extrados, intrados and simultaneous GFRP strengthening increased the ultimate load to be 12, 16 and 21 times that of the unstrengthened vault, respectively. The same full strengthening by steel bars raised the ultimate load of the unstrengthened vault by 3–8 times for the various schemes. Explanation of this enhancement was given by researchers that when the FRP reinforcement is placed at the intrados, it contributes to holding the bricks together. Experimental research by Valluzzi et al. [50] showed that arches strengthened at the extrados exhibited brittle failure which can be resolved by optimizing the quantity of applied FRP and increasing the amount of material near the abutments. Valluzzi et al. reported irregular distribution of stresses in the zone under the CFRP reinforcement due to the high stress level in the small width strips of high Young's modulus, which affects the overall vault capacity [50].

7. Conclusions

This paper presented simplified nonlinear analysis of masonry flat and vaulted elements externally strengthened by using different techniques. An experimental program was conducted and the numerical results are compared with the experimental outcomes to investigate the feasibility of the modeling for representing the structural behavior of masonry walls and vaults strengthened with different schemes. The main conclusions drawn from this study may be summarized in the following points.

- Unreinforced masonry wallets strengthened by externally bonded GFRP sheets and tested in diagonal compression until failure showed 100% increase in ultimate load compared to unstrengthened wallets.
- Use of steel reinforcement bars, FRP externally bonded sheets and ferro-cement wire mesh are effective low cost methods for strengthening masonry vaults, as they increased the ultimate loads to 150%, 190% and 150% of the unstrengthened vaults, respectively. Strengthening with polymer mortar layer showed slight enhancement of 118%.
- External FRP strengthening nearly doubled the ultimate capacity of the tested unreinforced masonry walls and vaults and improved the failure mode. Other advantages such as ease of installation, small thickness, minimum intervention and reversibility make FRP an attractive alternative for traditional strengthening methods.

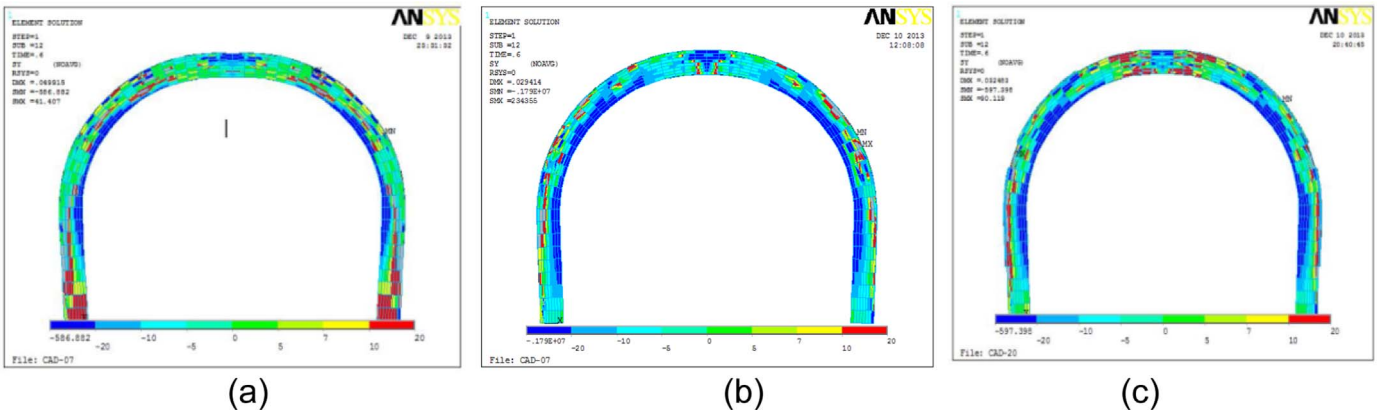

Fig. 16. Stresses (x10^{-2} MPa) in the vaults strengthened by a) steel reinforcement bars, b) GFRP sheets, c) ferro-cement wire mesh.

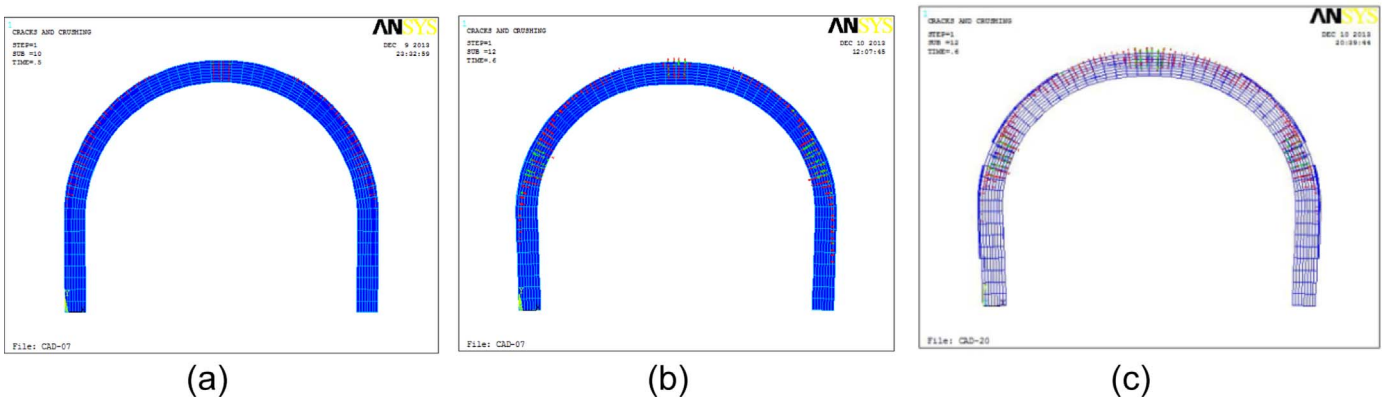

Fig. 17. Crack patterns in the vaults strengthened by a) steel reinforcement bars, b) GFRP sheets, c) ferro-cement wire mesh.

- Retrofitting by externally applied FRP can be used to control the opening hinges in the extrados of the masonry vaults, and can also be used to upgrade the ultimate, load carrying capacity and the ductility of the vaulted structures. Arrangement of the FRP externally adhered reinforcement should follow the expected vault failure mode.
- Numerical modeling and nonlinear analysis were done by using a commercially available computer program (ANSYS), which renders the approach applicable by practicing designers.
- The results of the numerical study showed good agreement with the results of the laboratory tests as regards crack patterns and failure mechanisms for all models and for the maximum load and the corresponding deformation for most cases.
- The adopted numerical modeling may thus be regarded as a reliable tool to explore and compare the different strengthening schemes for masonry walls and vaults and predict the failure mode, ultimate load-carrying capacity and safety level of such strengthened structures.
- A parametric study using the presented approach was made where several strengthening configurations were numerically modeled and analysed in order to reach the optimum one.
- Numerical results show that all strengthening placed at the vaults intrados result in higher peak load values compared with placement at the extrados, for all schemes considered.

Table 4
Numerically evaluated failure loads for vaults with full strengthening.

Strengthening location Strengthening technique	Extrados Failure load (kN)	Intrados Failure load (kN)	Extrados + intrados Failure load (kN)
No strengthening	8.0	–	–
Steel bars 6 mm diam.@ 250 mm	32	36	36
Steel bars 6 mm diam.@ 125 mm	34	38	38
Steel bars 12 mm diam.@ 250 mm	44	62	68
Steel bars 12 mm diam.@ 125 mm	48	70	75
GFRP sheets- 1 layer	92	130	160
GFRP sheets- 2 layers	95	135	176
CFRP strips @ 250 mm	70	85	85
CFRP strips @ 125 mm	90	95	95

- Simultaneous extrados and intrados reinforcement gave very slight increase over strengthening at intrados only for steel bars and nearly no increase for FRP strengthening.
- The previous conclusion is quite satisfactory, as in practical cases usually the vault intrados is luckily accessible, while strengthening

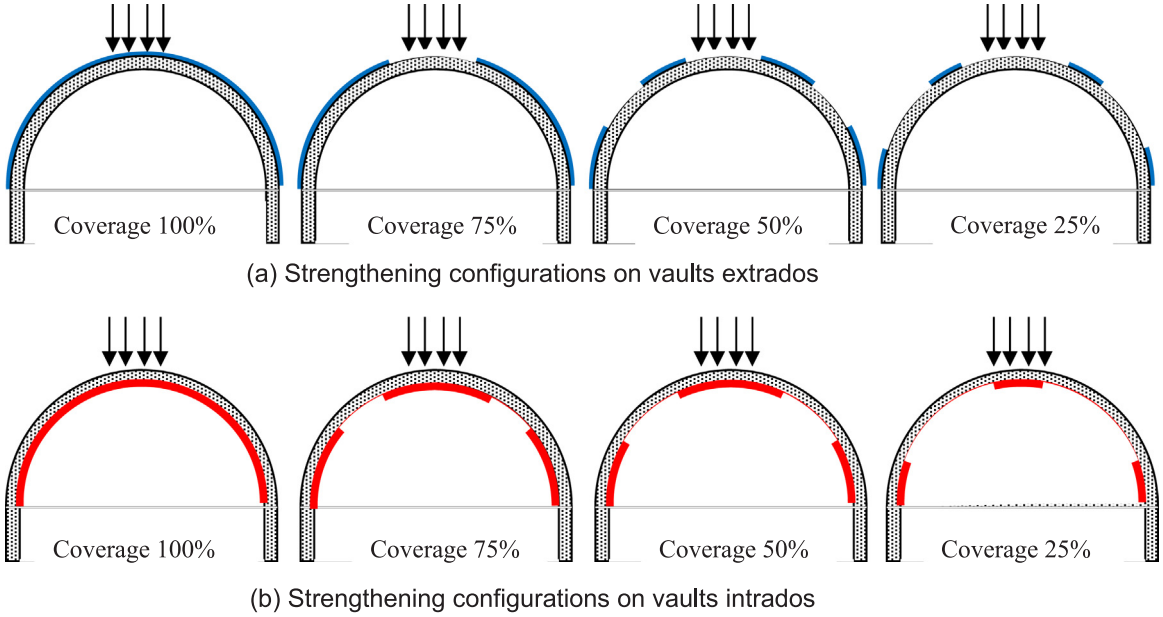

Fig. 18. Strengthening configurations externally applied on vaults a) extrados and b) intrados.

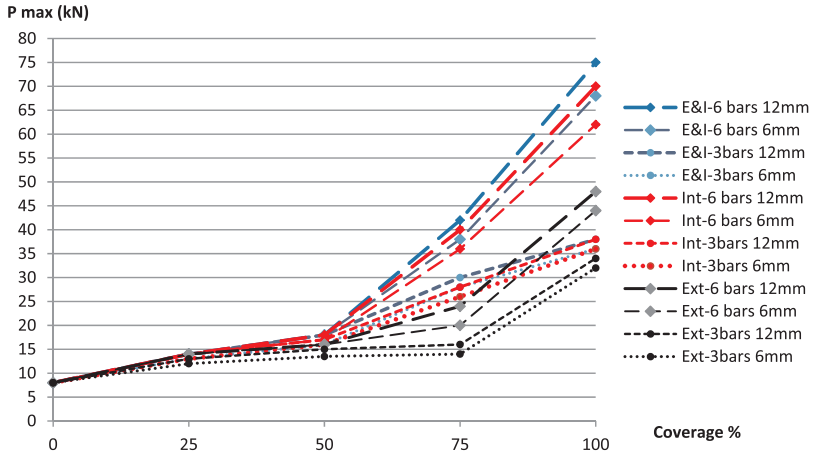

Fig. 19. Maximum loads for vaults strengthened with steel bars with different configurations.

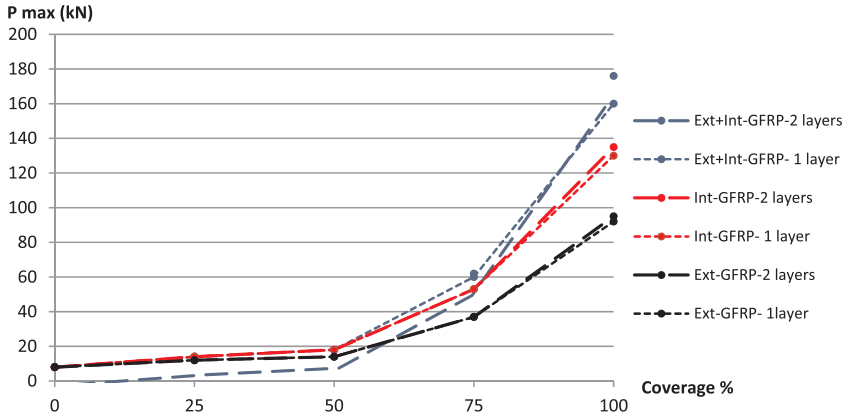

Fig. 20. Maximum loads for vaults strengthened with GFRP with different configurations.

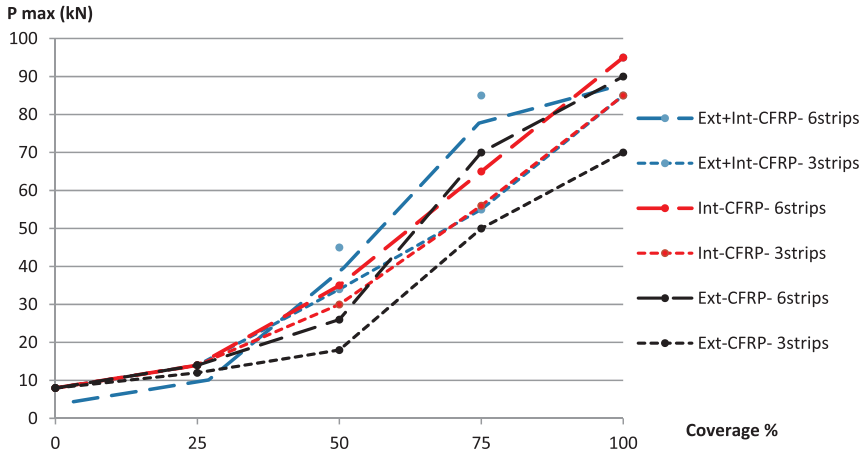

Fig. 21. Maximum loads for vaults strengthened with CFRP strips with different configurations.

the vault extrados requires construction works to remove overlays or roof.

- Increasing the strengthening amount (steel area or thickness of FRP) has minor effect on increasing the load carrying capacity, while better distribution, more length causes higher increase.
- Location of the strengthening has the most obvious effect on raising the carrying capacity, improving ductility and improving the failure mode. Strengthening by FRP sheets covering only half the vaults intrados surface at certain locations managed to increase the ultimate load to 2.25 times that of unstrengthened vault, and if coverage is increased to 75% the peak load reached 6.6 times that of unstrengthened vault.
- As a result of conducted experimental and numerical studies, the authors recommend that GFRP sheets or CFRP strips should be applied at selected locations of the vault intrados, with the following aims: reduction of tensile stress in masonry, limiting deformation and reduction of crack width.
- This work may be extended to simulate accurately the bond between masonry and FRP or steel elements rather than the assumption of full bond adopted in the present work. Further numerical investigations are needed to better model the bond and transfer of tangential stresses between the masonry and the strengthening elements.
- The research could be extended to allow for use of other strengthening techniques such as prestressed FRP laminates, post-tensioning steel or FRP rods, and other.

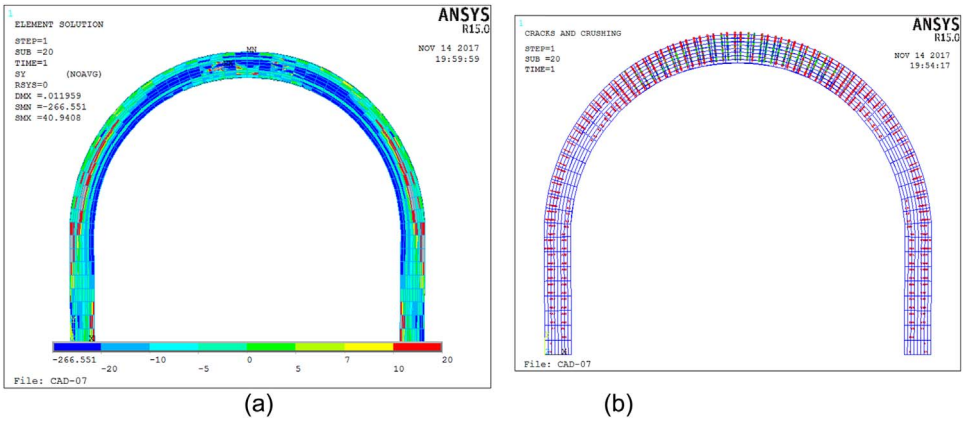

Fig. 22. Vaults with full strengthening on both extrados and intrados by 6 steel bars a) stresses before failure and c) crack pattern.

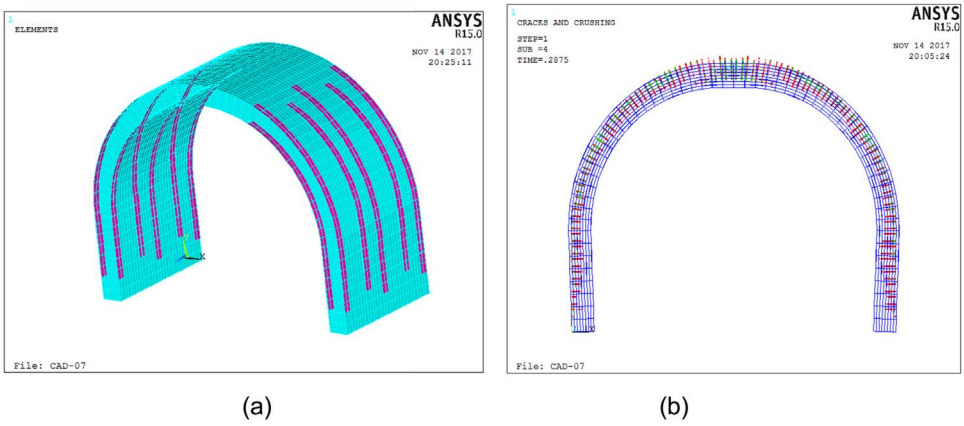

Fig. 23. Vaults with strengthening by 6 CFRP strips on both extrados and intrados a) finite element mesh and b) crack pattern.

- Further research is suggested to study the nonlinear behavior of masonry structures subject to dynamic loads such as impact, cyclic loading, vibrations or earthquakes.

References

[1] P.B. Lourenco, Computations on historic masonry structures, Prog. Struct. Mat. Eng. 4 (3) (2002) 301–319.
[2] P. Roca, M. Cervera, G. Gariup, L. Pelà, Structural analysis of masonry historical constructions, classical and advanced approaches, Arch. Comput. Methods Eng. 17 (3) (2010) 299–325.
[3] A. D'Ambrisi, M. Valentina, M. Marco, Seismic assessment of a historical masonry tower with nonlinear static and dynamic analyses tuned on ambient vibration test, Eng. Struct. 36 (2012) 210–219.
[4] F. Clementi, V. Gazzani, M. Poiani, S. Lenci, Assessment of seismic behavior of heritage masonry buildings using numerical modeling, J. Build. Eng. 8 (2016) 29–47.
[5] ANSYS v.12, ANSYS® Nonlinear Analysis Computer Program, Release 12.0, Theory Reference Manual, ANSYS Inc., Canonsburg, PA, USA.
[6] T. El-Salakawy, Response of Masonry Structures Strengthened by Different Techniques, Ph.D. Thesis Benha University, Egypt, 2015.
[7] A.W. Page, Finite element model for masonry, J. Struct. Div. ASCE 104 (8) (1978) 1267–1285.
[8] P.B. Lourenço, Computational Strategies for Masonry Structures, Ph.D. Dissertation Delft University of Technology, Netherlands, 1996.
[9] P.B. Lourenço, G. Milani, A. Tralli, A. Zucchini, Analysis of masonry structures: review of and recent trends of homogenization techniques, Can. J. Civ. Eng. 34 (2007) 1443–1457.
[10] P. Roca, M. Cervera, L. Pelà, R. Clemente, M. Chiumenti, Continuum FE models for the analysis of Mallorca Cathedral, Eng. Struct. 46 (2013) 653–670.
[11] G. Milani, Simple homogenization model for the non-linear analysis of in-plane loaded masonry walls, Comp. Struct. 89 (2011) 1586–1601.
[12] F. Peña, P.B. Lourenço, N. Mendes, D.V. Oliveira, Numerical models for the seismic assessment of an old masonry tower, Eng. Struct. 32 (5) (2010) 1466–1478.
[13] C.C. Spyrakos, P.D. Kiriakopoulos, E. Smyrou, Seismic strengthening of the historic church of St Helen and Constantine in Piraeus, in: Proceedings of the 3rd ECCOMAS Thematic Conference on Computational Methods in Structural Dynamics and Earthquake Engineering COMPDYN 2011, Corfu, Greece, May, 2011.
[14] M. Betti, A. Vignoli, Numerical assessment of the static and seismic behaviour of the basilica of Santa Maria all'Impruneta (Italy), Constr. Build. Mater. 25 (2011) 4308–4324.
[15] F. Ceroni, M. Pecce, S. Sica, A. Garofano, Assessment of seismic vulnerability of a historical masonry building, Build 2 (2012) 332–358.
[16] O.A. Kamal, G.A. Hamdy, T.S. El-Salakawy, Nonlinear analysis of historic and contemporary vaulted masonry assemblages, HBRC J. Elsevier 10 (2014) 235–246.
[17] M. Betti, L. Galano, A. Vignoli, Time-history seismic analysis of masonry buildings: a comparison between two non-linear modelling approaches, Build 5 (2015) 597–621.
[18] H.B. Kaushik, D.C. Rai, S.K. Jain, Stress-strain characteristics of clay brick masonry under uniaxial compression, J. Mater. Civ. Eng. ASCE 19 (9) (2007) 728–739.
[19] D. García, J.T. San-José, L. Garmendia, R. San-Mateos, Experimental study of traditional stone masonry under compressive load and comparison of results with design codes, Mater. Struct. 45 (7) (2012) 995–1006.
[20] W. McNary, D. Abrams, Mechanics of masonry in compression, J. Struct. Eng. 111 (4) (1985) 857–870.
[21] R. Bennett, K. Boyd, R. Flanagan, Compressive properties of structural clay tile prisms, J. Struct. Eng. 123 (7) (1997) 920–926.
[22] L. Binda, C. Tiraboschi, S. Abbaneo, Experimental research to characterise masonry materials, Mason. Int. 10 (3) (1997) 92–101.
[23] B. Ewing, M. Kowalsky, Compressive behaviour of unconfined and confined clay brick masonry, J. Struct. Eng. 130 (4) (2004) 650–661.
[24] A. Costigan, S. Pavía, O. Kinnane, An experimental evaluation of prediction models for the mechanical behavior of unreinforced, lime-mortar masonry under compression, J. Build. Eng. 4 (2015) 283–294.
[25] EN1996-1and 2: 2005, Eurocode 6- Design of masonry structures. Part1-1:- General rules for buildings—reinforced and unreinforced masonry, Design of masonry structures. Design Considerations, Selection of Materials and Execution of Masonry. European Committee for Standardisation CEN, Brussels, 2006.
[26] T. Paulay, M.J.N. Priestley, Seismic Design of Reinforced Concrete and Masonry Buildings, Wiley-Interscience, NewYork, 1992.
[27] Z. Radovanovic, R.S. Grebovic, S. Dimovsk, N. Serdar, N. Vatin, V. Murgul, Mechanical properties of masonry walls – analysis of the test results, Procedia Eng. 117 (2015) 865–873.
[28] R. Chmielewski, L. Kruszka, Application of selected modern technology systems to strengthen the damaged masonry dome of historical St. Anna's Church in Wilanów (Poland), Case Stud. Constr. Mater. 3 (2015) 92–101.
[29] P. Foraboschi, Versatility of steel in correcting construction deficiencies and in seismic retrofitting of RC buildings, J. Build. Eng. 8 (2016) 107–122.
[30] A.H. Akhaveissy, G. Milani, A numerical model for the analysis of masonry walls in-plane loaded and strengthened with steel bars, Int. J. Mech. Sci. 72 (2013) 13–27.
[31] R. Islam, Inventory of FRP Strengthening Methods in Masonry Structures (Master Thesis), Technical University of Catalonia, Italy, 2008.

[32] P. Michelis, C. Papadimitriou, G.K. Karaiskos, D.C. Papadioti, C. Fuggini, Seismic and vibration tests for assessing the effectiveness of GFRP for retrofitting masonry structures, Smart Struct. Syst. 9 (3) (2012) 207–230.
[33] C.R. Willis, R. Seracino, M.C. Griffith, Out-of-plane strength of brick masonry retrofitted with horizontal NSM CFRP strips, Eng. Struct. 32 (2) (2010) 547–555.
[34] C. Papanicolaou, T. Triantafillou, M. Lekka, Externally bonded grids as strengthening and seismic retrofitting materials of masonry panels, Constr. Build. Mater. 25 (2) (2011) 504–514.
[35] M. El-Diasity, H. Okail, O. Kamal, M. Said, Structural performance of confined masonry walls retrofitted using ferrocement and GFRP under in-plane cyclic loading, Eng. Struct. 94 (2015) 54–69.
[36] F. Monni, E. Quagliarini, S. Lenci, F. Clementi, Dry masonry strenghtening through basalt fibre ropes: experimental results against out-of-plane actions, Key Eng. Mater. (2015) 624.
[37] E. Bernat-Maso, L. Gil, P. Roca, Numerical analysis of the load-bearing capacity of brick masonry walls strengthened with textile reinforced mortar and subjected to eccentric compressive loading, Eng. Struct. 91 (2015) 96–111.
[38] A. Gabor, A. Benanni, E. Jacquelin, F. Lebon, Modelling approaches of the in-plane shear behaviour of unreinforced and FRP strengthened masonry panels, Compos. Struct. 74 (2006) 277–288.
[39] E. Grande, M. Imbimbo, E. Sacco, Finite element analysis of masonry panels strengthened with FRPs, Compos. Part B 1 (2013) 1296–1309.
[40] M. Basili, G. Marcari, F. Vestroni, Nonlinear analysis of masonry panels strengthened with textile reinforced mortar, Eng. Struct. 113 (2016) 245–258.
[41] F. Ceroni, A. Garofano, M. Pecce, Finite element modelling of masonry panels reinforced with FRP grids, in: National conference ANIDIS, Padova, Italy, 2013.
[42] S.S. Mahini, Smeared crack material modeling for the nonlinear analysis of CFRP-strengthened historical brick vaults with adobe piers, Constr. Build. Mater. 74 (2015) 201–218.
[43] J. Szołomicki, P. Berkowski, J. Barański, Computer modeling of masonry cross vaults strengthened with fiber reinforced polymer strips, Arch. Civ. Mech. Eng. (2015) 751–766.
[44] C. Mazzotti, F.S. Murgo, Numerical and experimental study of GFRP-masonry interface behavior: bond evolution and role of the mortar layers, Compos. Part B 75 (2015) 212–225.
[45] K.J. Willam, E.P. Warnke, Constitutive model for the triaxial behavior of concrete, in: Proceedings of the International Association for Bridge and Structural Engineering, ISMES, Bergamo, Italy, 1975.
[46] A.W. Page, The biaxial compressive strength of brick masonry, Proc. Inst. Civ. Eng. 71 (3) (1981) 893–906.
[47] ECP 204-2005, Egyptian Code for Design and Construction of Masonry Structures, Ministry of Housing and Urban Communities, Egypt, 2005.
[48] ASTM E519-02, Standard test method for diagonal tension (shear) in masonry assemblages, American Society for Testing and Materials ASTM E 519–02, Philadelphia, 2002.
[49] D.V. Oliveira, L. Basilio, P.B. Lourenço, Experimental behavior of FRP strengthened masonry arches, J. Comp. Constr. 14 (3) (2010) 312–322.
[50] M.R. Valluzzi, M. Valdemarca, C. Modena, Behavior of brick masonry vaults strengthened by FRP laminates, J. Compos. Constr. 5 (3) (2001) 165–169.
[51] Sandeep, M.V. Renukadevi, S. Manjunath, Somanath, Influence of reinforcement on the behavior of hollow concrete blocks masonry prism under compression – an experimental and analytical approach, Int. J. Res. Eng. Technol. (2013) 106–110.
[52] I. Basilio, D. Oliveira, P. Lourenço, Optimal FRP strengthening of masonry arches, in: Proceedings of the 13th International Brick and Block Masonry Conference, Amsterdam, July 4-7.